Journal Pre-proof

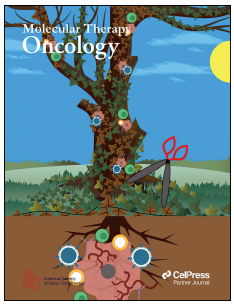

An αvβ6 specific precision virotherapy expressing bispecific immune cell activators induces immune cell activation and mediates tumour cell death.

Rebecca J. Bayliss, Luned M. Badder, James Davies, Andrew Robinson, Mona Pissarreck, Simon Kollnberger, Alan L. Parker

PII: S2950-3299(25)00086-4

DOI: https://doi.org/10.1016/j.omton.2025.201017

Reference: OMTON 201017

To appear in: *Molecular Therapy: Oncology*

Received Date: 27 March 2025

Revised Date: 7 June 2025

Accepted Date: 23 June 2025

Please cite this article as: Bayliss RJ, Badder LM, Davies J, Robinson A, Pissarreck M, Kollnberger S, Parker AL, An αvβ6 specific precision virotherapy expressing bispecific immune cell activators induces immune cell activation and mediates tumour cell death., *Molecular Therapy: Oncology* (2025), doi: https://doi.org/10.1016/j.omton.2025.201017.

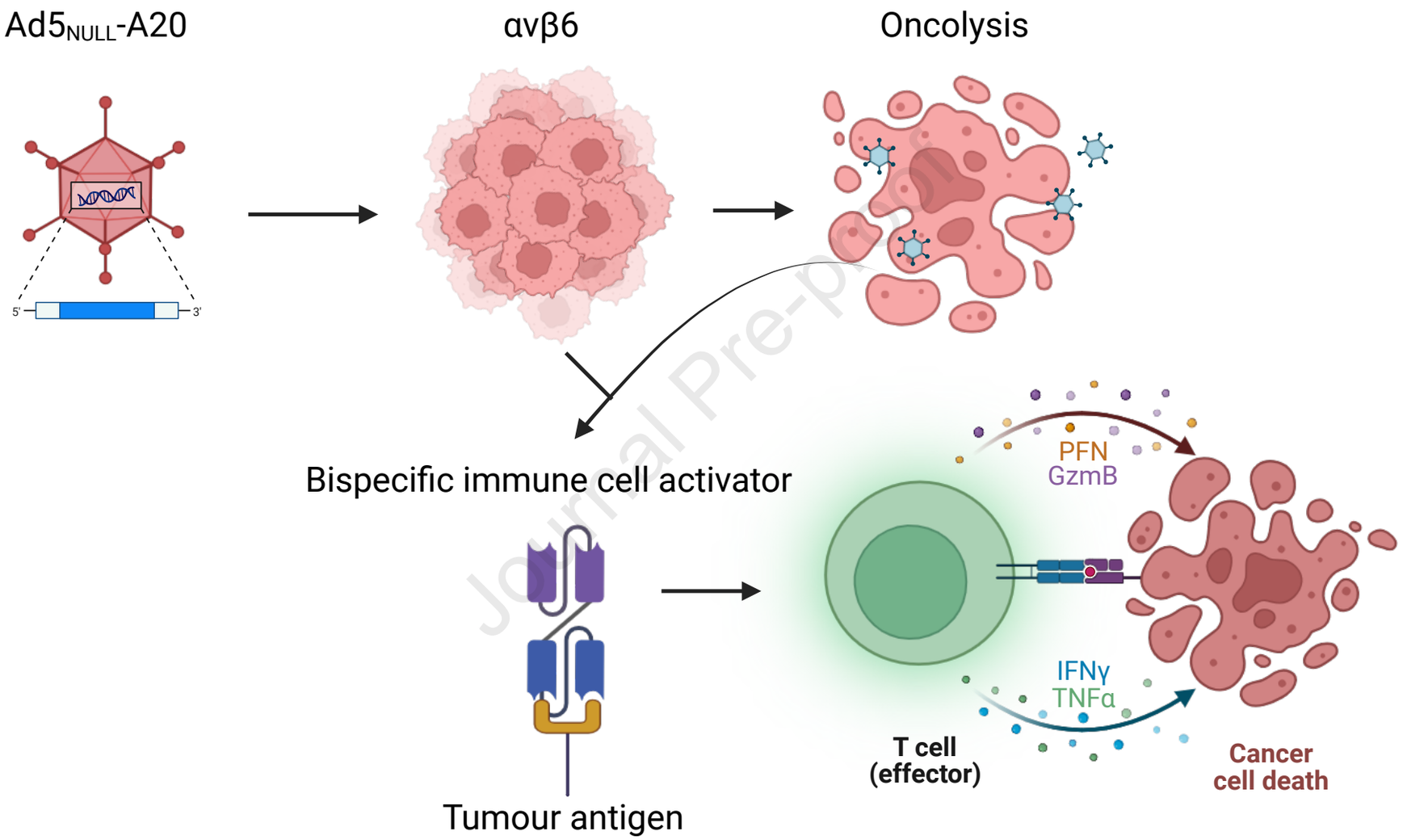

An αvβ6 specific precision virotherapy expressing bispecific immune cell activators induces immune cell activation and mediates tumour cell death.

Rebecca J. Bayliss[1], Luned M. Badder[1], James Davies[1], Andrew Robinson[1], Mona Pissarreck[1], Simon Kollnberger[2], Alan L. Parker[1,3*]

[1] Department of Cancer and Genetics, School of Medicine, Cardiff University, Cardiff, CF14 4XN, UK.

[2] Department of Infection and Immunity, School of Medicine, Cardiff University, Cardiff, CF14 4XN, UK.

[3] Systems Immunity University Research Institute, School of Medicine, Cardiff University, Cardiff, CF14 4XN, UK.

*** Corresponding author:**
Professor Alan L Parker FLSW
Email: ParkerAL@Cardiff.ac.uk
Tel: +44 (0) 2922510231

Short title: αvβ6 integrin targeted "in tumour immunotherapy".

Abstract

$Ad5_{NULL}$-A20 is an Adenovirus type 5 based precision virotherapy engineered to selectively target αvβ6 positive tumours. Bispecific immune cell activators (BICA) bind both an immune cell receptor and tumour cell-associated antigen (TAA) in tandem to induce a tumour-specific immune response. Combining the selectivity and oncolytic properties of $Ad5_{NULL}$-A20 with the potency of BICA will create a more tolerated, enduring immune cell response limited to tumour sites, reducing off target effects and dose limiting toxicities. We developed multiple BICA targeting T-cells via CD3, Natural killer (NK cells) via CD16/NKG2D receptors and TAA Epidermal growth factor receptor (EGFR) and Major histocompatibility complex related chain A (MICA). *In vitro* studies establish that $Ad5_{NULL}$-A20 BICA in αvβ6 tumour cells, results in T-cell and NK activation at tumour sites and a loss of tumour cell viability. *Ex vivo* studies validate these findings demonstrating a significant and rapid reduction in growth of patient-derived 3D tumour organoids transduced with oncolytic $Ad5_{NULL}$-A20-BICA in the presence of T- or NK- cells. $Ad5_{NULL}$-A20 expressing BICA can produce a potent immune response resulting in tumour eradication. This approach has significant translational potential to develop a novel cancer therapeutic for clinical success.

Introduction

Solid tumours are composed of heterotypic cell masses, connective-tissue, and immune cells that communicate between tight and gap junctions to enable the formation of a tumour microenvironment (TME). A vast range of immunotherapies have been designed to regulate immunostimulatory molecules within the TME to impede tumour immune escape. Often a combination of immunotherapies is used in the treatment of solid tumours to overcome tumour evasion strategies [1].

Oncolytic viruses selectively replicate and lyse tumour cells resulting in release of virus and tumour specific antigens leading to immune cell infiltration at tumour sites. This, in combination with the ability to carry transgenes to tumour sites makes them an attractive option for the development of cancer therapeutics [2]. Oncolytic Adenovirus type 5 (Ad5) has a good safety record and is permissive to transgene insertion, however its efficacy as a cancer therapeutic is limited by off-target effects due to poor selectivity. To overcome such limitations, we previously developed $Ad5_{NULL}$-A20 incorporating detargeting mutations into each of the capsid proteins, ablating native receptor binding and reducing off-target toxicities. $Ad5_{NULL}$-A20 was retargeted via insertion of a 20-mer A20 peptide into the fiber knob HI loop to enable selective uptake into αvβ6 positive tumours [3].

Bispecific immune cell activators (BICA) are traditionally composed of two single-chain variable fragments (scfv) from two individual monoclonal antibodies connected via a tandem flexible linker. BICA are designed to simultaneously bind an immune cell receptor and a tumour-associated antigen resulting in the formation of MHC-independent cytolytic synapse. The formation of the synapse leads to cytotoxic release of perforin and granzyme B resulting in tumour cell lysis [4]. BICA have shown encouraging clinical results for haematological malignancies, in 2014 the first BICA Blinatumomab® (CD3×CD19) was approved to treat relapsed/refractory lymphoblastic leukaemia [5]. Treatment of solid tumours with BICA has proven to be more challenging due to limited tumour penetration and poor efficacy in the presence of the TME. The continuous systemic delivery of BICA leads to the occurrence of on-target off-tumour severe adverse events including cytokine release syndrome (CRS),

neurotoxicity hepato- and cardiotoxicities [6]. To date, only Tarlatamab (DLL3xCD3) has been granted FDA approval for the treatment of small cell lung cancer (FDA), therefore improvements to the delivery of BICA is paramount to significantly improve outcomes.

To enhance therapeutic potential of $Ad5_{NULL}$-A20 in αvβ6 positive solid epithelial tumours we designed a range of BICA to be incorporated into the $Ad5_{NULL}$-A20 genome allowing the release of the therapeutic at tumour sites. By harnessing the immune response generated by oncolytic infection of tumour cells we intended to redirect and activate immune cells via the release of BICA within the local TME. This approach enables multiple tumour antigens to be targeted generating an effective and sustained immune response at tumour sites, significantly overcoming issues associated with tumour cell heterogeneity. In addition, restricting the release of the BICA at tumour sites using a targeted virotherapy we aim to circumvent the toxicities seen via current systemic administration, limiting damage to healthy tissue to enhance safety profile of BICA.

These studies investigate the ability of a precision virotherapy, $Ad5_{NULL}$-A20, to transduce αvβ6 cancer cells and produce BICA immunostimulatory molecules. Secreted BICA generated an effective immune response and reduced tumour growth in EGFR/MICA positive tumours *in vitro*. We confirmed this activity in pancreatic patient derived models *ex vivo*, demonstrating a significant and rapid reduction in tumour cell growth in the presence of T- and NK cells when transduced with Oncolytic $Ad5_{NULL}$-A20-BICA ($OAd5_{NULL}$-A20-BICA).

The findings presented here support the development of $OAd5_{NULL}$-A20-BICA as a therapeutic candidate in the treatment of more difficult to treat solids tumours. This approach enables targeting of abundant tumour associated antigens with significant translational potential.

Results

Generation of $Ad5_{NULL}$-A20-BICA with oncolytic and immunogenic properties

Each BICA was designed to express a human CD33 signaling peptide at the N-terminus to enable secretion from cells. Constructs containing two single-chain-variable fragments (scfv) a variable light (VL) and variable heavy (VH) chain are displayed in a VL-VH-VH-VL format with connecting G4S N-linkers (**Table S2**). A V5 tagged protein at the C-terminus allows detection of scfv-scfv constructs. In the instance of a scfv-ligand and scfv-receptor format, the ligand/extracellular domain of the receptor replaces the scfv domain related to the desired target. Ligand-Ligand format connects two ligands via a G4S N-linker. CD16scfv, Major histocompatibility complex-related chain A (MICA) ligand and Natural killer group 2D (NKG2D) scfv target CD16 or NKG2D receptor (NKG2Drp) present on NK cells. CD3scfv target T-cells via the CD3 receptor. Tumour antigens are in turn targeted via binding to either MICA via NKG2Drp or Epidermal Growth Factor Receptor (EGFR) via EGFR scfv or Epidermal Growth Factor (EGF) ligand (**Fig. 1A**).

BICA were recombineered [7] into replication-deficient and oncolytic Ad5 and $Ad5_{NULL}$-A20 BACs and competent viruses generated (**Table S3-4**). To determine if incorporation of the BICA transgenes detrimentally effect the virus's oncolytic properties three cancer cell lines: Panc0403 (αvβ6+), KYSE30 (αvβ6+) and PT45 (αvβ6-) with variable αvβ6 expression (**Fig. S1**) were transduced with $OAd5_{NULL}$-A20-BICA (**Fig. 1B-D**). All tested virotherapies displayed similar levels of oncolysis to $OAd5_{NULL}$-A20 alone. Immunogenic cell death is requisite for the accumulation of Damage-associated molecular patterns (DAMPs) such as ATP and HMGB1 to recruit and activate antigen presenting cells (APC). One major advantage of oncolytic viruses in the treatment of cancer is the ability to induce immunogenic cell death at tumour sites. To establish if $OAd5_{NULL}$-A20-BICA induce immunogenic cell death in αvβ6+ve cells, HMGB1 release was quantified after 24 hours transduction (**Fig. 1E**). An increase in HMGB1 between 30-50 ng/mL was evident in all $Ad5_{NULL}$-A20-BICA transduced cells equivalent or greater than the $Ad5_{NULL}$-A20 control. Extracellular ATP release was evident for all $OAd5_{NULL}$-A20-BICA peaking at 60-

64 hours post-infection and gradually declining at 96 hours, coinciding with cell death (**Fig 1F**). These data indicate that incorporation of bispecific transgenes does not significantly impact oncolytic nor immunogenic properties of $OAd5_{NULL}$-A20, ensuring optimal performance of the precision virotherapy at tumour sites.

BICA activation of immune cells is dependent on EGFR and MICA tumour antigen binding.

Expression and secretion of BICA from transduced cells is paramount to their function to activate immune cells at tumour sites. Supernatants containing secreted BICA, and cell lysates were processed for western blotting. Variable expression of all BICA molecules was evident within cell lysates. The majority of BICA were secreted at detectable levels, except for CD16/CD3scfv-NKG2Drp (**Fig. 2A and Fig S2**).

Binding to respective TAA was assessed by incubating supernatants containing BICA on EGFR/MICA positive or negative cell lines (**Fig. 2B and Fig. S3-4**). Binding to EGFR or MICA was evident for eight out of ten BICA tested when compared to TAA negative cells. CD16scfv-NKG2Drp showed no binding to MICA, whereas EGF-MICA did not show any binding to EGFR.

The biological activity and specificity of CD3-BICA were initially evaluated *in vitro* using Jurkat NFκB GFP reporter cells incubated with the various CD3-BICA supernatants (**Fig. 2C-D**) in the presence or absence of EGFR or MICA (**Fig. S3**). NFκB driven transcription of GFP resulting from binding to CD3 was significantly increased in the presence of CD3-EGFRscfvs, CD3scfv-EGF and CD3scfv-NKG2Drp, dependent on the presence of TAA. No GFP was evident in the absence of TAA nor in the presence of an 'off-target' BICA. In the case of CD3-EGFRscfvs GFP induction was higher than the positive control CD3/CD28 beads (**Fig 2C**). Using a similar approach, NK cells targeting BICA supernatants were co-cultured with NK derived cells in the presence or absence of EGFR (**Fig. 2E**). A substantial increase in CD56+CD107a+ cells, indicative of NK cell activation, was evident in five of six BICA tested. The exception being EGF-MICA where no increase in CD107a was detected.

This data confirms that T-cell and NK cell BICA specifically and efficiently bind to tumour antigens in an EGFR/MICA dependent manner and engage with target immune cells to induce an effective immune response. Seven of the BICA evaluated were selected for further analysis: CD3-EGFRscfvs, CD3scfv-EGF, CD16-EGFRscfvs, CD16scfv-EGF, EGFRscfv-MICA, EGFR-NKG2Dscfvs and NKG2Dscfv-EGF. Although secretion of CD3scfv-NKG2Drp was not evident (**Fig. 2A**), the BICA performed well in other assays leading to the decision to take it forward for further testing. EGF-MICA was detected via western blot using the MICA antibody; however, it failed to show evidence of binding when targeted to EGFR, suggesting the EGF ligand was not binding as expected. Similarly, CD16scfv-NKG2Drp failed to show any binding or functionality, likely due to poor protein expression and/or processing. Therefore, these were both removed from further analysis.

$Ad5_{NULL}$-A20 CD3-BICA induce T-cell activation and immune mediated tumour death.

$Ad5_{NULL}$-A20 selectively targets $\alpha v\beta 6$ positive solid epithelial tumors, therefore three cancer cell lines representing a range of epithelial solid tumour types were selected: BT20 (triple-negative breast cancer), KYSE30 (esophageal squamous cell carcinoma) and Panc0403 (pancreatic adenocarcinoma). Each cell line overexpresses $\alpha v\beta 6$, required for $Ad5_{NULL}$-A20 transduction, and EGFR and MICA (including other NKG2D ligands) required for BICA activation (**Fig. S1, Table S1**), therefore possess the required characteristics to demonstrate T-cell activation and tumour cell lysis by CD3-BICA. CD25 and CD69 early activation markers were used to determine activation of the T-cells via CD3 in CD3-BICA transduced cells (**Fig. 3A-B**). A clear increase in both CD69 and CD25 was evident in CD4+ and CD8+ T-cell populations transduced with $Ad5_{NULL}$-A20-CD3-BICA compared to controls. CD3-EGFRscfvs and CD3scfv-EGF saw the greatest increase (CD69 98-99%, CD25 60-80%) with activation, in many cases, equivalent to the positive control. In the instance of CD3scfv-NKG2Drp, activation was lower, particularly in the replication-deficient virotherapies, this is in line with the fact that CD3-EGFRscfvs and CD3scfv-EGF is more highly expressed and secreted than CD3scfv-NKG2Drp (**Fig. 2a**) in cells. A similar pattern of activation was evident in both KYSE30 and Panc0403 cells. However, Panc0403

transduced with replication-deficient $Ad5_{NULL}$-A20-BICA RD had lower CD69 positive T-cells compared to BT20 and KYSE30.

Intracellular IFNγ increased in the presence of $Ad5_{NULL}$-A20-CD3-BICA transduced cells compared to controls, with CD3-EGFRscfvs and CD3scfv-EGF performing better than CD3scfv-NKG2Drp. Intracellular IFNγ was more elevated in CD8+ T-cells than CD4+ T-cells across the board, with BT20 cells seeing a greater overall increase in IFNγ positive cells than KYSE30 or Panc0403 (**Fig. 3C**). T-cell proliferation over five days also saw an increase in the CD3+ T-cell division index compared to controls (**Fig. 3D**). Panc0403 transduced with replication-deficient $Ad5_{NULL}$-A20 CD3-BICA had notably reduced proliferation compared to the oncolytic.

A dramatic loss of cell viability (100-75%) in both replication-deficient (**Fig. 3E**) and oncolytic (**Fig. 3F**) cells transduced with $Ad5_{NULL}$-A20 CD3-BICA was evident between 1-5 days co-culture, except for Panc0403 CD3scfv-NKG2Drp which only reduced cell viability by 33% compared to untreated cells. The reduced activity of $Ad5_{NULL}$-A20 CD3-BICA RD in Panc0403 cells is attributed to low secretion levels of the BICA in this cell line which is overcome by the use of an oncolytic alternative.

Altogether, these data provide evidence that $Ad5_{NULL}$-A20 CD3-BICA virotherapies can, when transduced into αvβ6 positive tumour cells, release CD3-BICA at the tumour site resulting in activation of T-cells and down-stream proliferation amounting to a potent immune response at tumour sites to induce immune mediated lysis of tumour cells.

$Ad5_{NULL}$-A20 CD16-BICA induce NK activation and immune mediated tumour death.

CD107a or lysosome associated membrane protein-1 (LAMP-1) is a marker for degranulation of NK cells to determine cytotoxic activity, therefore αvβ6 positive cells were transduced with $Ad5_{NULL}$-A20 expressing NK-BICA and co-cultured with PBMCs. A significant increase in NK degranulation was

evident in NK cell co-cultured with tumour cells transduced with $Ad5_{NULL}$-A20 CD16-EGFRscfvs (approx. 30-40%). CD16scfv-EGF producing cells saw a more modest increase of between 7-22% (**Fig. 4A**). Replication-deficient $Ad5_{NULL}$-A20 CD16-BICA showed reduced CD107+ levels in Panc0403 in comparison to the oncolytic as seen previously in the CD3-BICA.

Remaining constructs (EGFRscfv-MICA, EGFR-NKG2Dscfvs, NKG2Dscfv-EGF) saw no increase in CD107a degranulation over background levels (not shown). Further testing of supernatants containing BICA (**Fig. S5A-B**) showed an increase of CD107a+ positive cells (25-50%) when normalised to negative control BICA (**Fig. S5B**), with comparable results to initial screening (**Fig. 2E**), suggesting the BICA can bind and activate NK cells. We next evaluated this in the context of $Ad5_{NULL}$-A20-BICA transduction co-cultured with purified NK cells. A modest increase in CD107a+ cells was seen in replication-deficient transduced cells (10-15%) compared to untreated cells, suggesting low secretion levels of the BICA from transduced cells. In contrast, cells transduced with $OAd5_{NULL}$-A20-BICA saw an increase (40-45%) (**Fig. S5C**) equivalent to previous levels (**Fig. S5A**), however $OAd5_{NULL}$-A20 devoid of any transgene also induced an increase of around 30%. Taken together, these data suggest that EGFRscfv-MICA, EGFR-NKG2Dscfvs, NKG2Dscfv-EGF as standalone BICA can function by inducing NK cell cytotoxicity, however $OAd5_{NULL}$-A20 is also able to trigger NK degranulation and although the combination of the BICA does marginally increase the response, it is difficult to discern the benefits of the addition of the bispecific to $OAd5_{NULL}$-A20 alone.

TNFα and IFNγ play important roles in surveillance of tumour growth, therefore TNFα and IFNγ production from NK cells co-cultured with $Ad5_{NULL}$-A20 CD16-BICA transduced cells was measured by ELISA. IFNγ and TNFα levels increased in transduced BT20 cells with both replication-deficient and $OAd5_{NULL}$-A20 CD16-BICA compared to controls. CD16-EGFRscfv saw a greater increase in cytokine production (15-28 pg/mL) than CD16scfv-EGF which produced around 1-3-fold less IFNγ (**Fig. 4B**) and TNFα (**Fig. 4C**). KYSE30 and Panc0403 also saw a similar increase in IFNγ and TNFα production (50-480

pg/mL) in cells transduced with OAd5$_{NULL}$-A20 CD16-BICA, however, replication-deficient Ad5$_{NULL}$-A20 CD16-BICA cytokine production was noticeably lower (0-100 pg/mL) for both IFNγ and TNFα.

Cell viability was determined between 1-5 days co-culture with purified NK cells in the presence of Ad5$_{NULL}$-A20 CD16-BICA (**Fig. 4D-E**). A loss of cell viability over 95% was evident in cells transduced with OAd5$_{NULL}$-A20 CD16-EGFRscfvs, greater than Ad5$_{NULL}$-A20 alone, suggesting NK cell mediated killing of the cancer cells. Replication-deficient Ad5$_{NULL}$-A20 CD16-EGFRscfvs reduced cell viability between 60-90% dependant on cell line. Despite moderate increases in CD107a, TNFα and IFNγ for cells transduced with OAd5$_{NULL}$-A20 CD16scfv-EGF a 65% decrease in BT20 and KYSE30 viability was observed increasing to 100% in Panc0403. Replication-deficient Ad5$_{NULL}$-A20 CD16scfv-EGF reduced BT20 and KYSE30 viability by 30-40%, however >10% killing was seen in Panc0403.

Taken together these data indicate Ad5$_{NULL}$-A20 CD16-EGFRscfvs is a potent activator of NK cells inducing cytotoxicity and release of TNFα and IFNγ resulting in NK cell induced tumour cell death. Ad5$_{NULL}$-A20 CD16scfv-EGF, although functional, exhibits a reduced level of cytotoxicity and tumour cell death in comparison to CD16-EGFRscfvs due to low expression levels in cells (**Fig. 2A**), despite this, CD16scfv-EGF in the oncolytic background still has potential to be a viable BICA moving forward, therefore OAd5$_{NULL}$-A20 CD16-EGFRscfvs and CD16scfv-EGF were taken forward for further testing.

OAd5$_{NULL}$-A20 CD3-BICA induce T-cell mediated tumour cell death in an *ex vivo* human pancreatic organoid model.

3D patient-derived tumour organoids retain many phenotypic and genetic properties of parental tumours, making them a valuable tool for the screening of cancer therapeutics. Characterisation of PDAC organoids show expression the surface receptors αvβ6 and EGFR (**Fig. S6A**), both required for internalisation of Ad5$_{NULL}$-A20 and bispecific tumour antigen targeting, respectively, making them a suitable model for demonstrating the potency of OAd5$_{NULL}$-A20-BICA *ex vivo*. Negligible MICA was found on the surface of the organoids tested; however solubilised MICA was present in the supernatants at high levels in PDM38 and PDM36 (**Fig. S6C**).

PDAC organoids from three donors (**Table S5**) were transduced with $OAd5_{NULL}$-A20-CD3-BICA before co-culture with CD3+ T-cells. The anti-tumour activity of $OAd5_{NULL}$-A20 CD3-BICA was evaluated against untreated and $OAd5_{NULL}$-A20 transduced cells co-cultured with T-cells. T-cell killing of organoids transduced with $OAd5_{NULL}$-A20 CD3-BICA can be seen as early as 18 hours, peaking at 48 hours post-co-culture across the three co-cultures (**Fig. 5A**). Untreated cells and $OAd5_{NULL}$-A20 remain viable at this time point and continue to grow in the presence of the T-cells. Analysis of organoid images show a decrease in organoid roundness, synonymous with reduced organoid integrity, in organoids transduced with $OAd5_{NULL}$-A20 CD3-EGFRscfvs, CD3scfv-EGF and CD3scfv-NKG2Drp compared to controls (**Fig. 5B**). In addition, labelling of T-cells shows clear infiltration of the organoid cultures compared to controls (**Fig. S7**). Cell viability was measured at 72 hours post-infection confirming the enhanced cell death seen in $OAd5_{NULL}$-A20 CD3-BICA transduced organoids compared to $Ad5_{NULL}$-A20 alone (**Fig. 5C**). Luminex cytokine analysis of co-culture supernatants indicate heightened production of Granzyme B, TNFα, IFNγ, IL-2 and low levels of Fas ligand and perforin (**Fig. 5D**) suggestive of T-cell cytotoxicity. In contrast, IL-6 was not detectable within these samples and IL-10 was only detected in one sample (PDM38) at very low levels which was not consistent across samples.

$OAd5_{NULL}$-A20 CD16-BICA induce NK cell mediated tumour cell death in an *ex vivo* human pancreatic organoid model.

NK cell's ability to reduce tumour organoid growth in the presence of CD16-BICA was assessed over 4 days using the Incucyte. $OAd5_{NULL}$-A20 CD16-EGFRscfvs, CD16scfv-EGF induced comparable NK cell mediated killing of organoids with a distinct increase in cell death evident around 72 hours post co-culture when compared to untreated and $OAd5_{NULL}$-A20. As expected $OAd5_{NULL}$-A20 also induced NK cell killing of transduced organoids around 72 hours, with organoids appearing smaller, with a distinct loss of structure and integrity, however the rate of tumour cell regression was noticeably slower in the absence of CD16-BICA (**Fig. 6A**). In line with these observations a significant decrease in organoid roundness was evident in organoids transduced with $OAd5_{NULL}$-A20 CD16-BICA compared to controls

(**Fig. 6B**), in addition organoids viability was compromised compared to controls (**Fig. 6C**) in conjunction with an increase in Granzyme A and IFNγ (**Fig 6D**). In the context of an *ex vivo* organoid model $OAd5_{NULL}$-A20 CD16-EGFRscfvs and CD16scfv-EGF transduction results in NK cell mediated death suggesting that a targeted virotherapy in conjunction with a CD16-EGFR BICA can effectively inhibit tumour cell growth.

Overall, these data provide evidence that $OAd5_{NULL}$-A20 CD3/CD16-BICA actively increase T-cell and NK cell anti-tumour activity resulting in enhanced cell death in αvβ6/EGFR/MICA positive PDAC models, suggesting their therapeutic benefit in a wide range of solid tumours with the same phenotypic profile.

Discussion

The development of bispecific antibodies has revolutionised cancer immunotherapy, outperforming the clinical efficacy of monoclonal antibodies [8]. The non-IgG-like format results in a shorter half-life (2 hours) with better tissue-penetration, lower rate of resistance, less immunogenicity, and increased immune specificity [9–11]. However, these advances are limited for the treatment of solid tumours due to the necessity to administer via continuous intravenous infusion, resulting in off-target toxicities, potentially leading to cytokine release syndrome (CRS) in patients [12].

The combination of BICA with oncolytic virotherapies enables the generation of BICA *in situ* offering many therapeutic advantages including selective replication in tumour cells reducing damage to healthy tissue and promoting tumour infiltrating lymphocytes (TILS) and remodelling and evasion of the immunosuppressive TME. Introduction of a dual modality of tumour cell killing by oncolysis or BICA encourages penetration of OV into solid tumours, targeting heterogenous tumours, and reducing systemic toxicities by restricting BICA production to transduced cancer cells whilst overcoming limitations of the BICA short half-life [13]. $Ad5_{NULL}$-A20 offers additional benefits by selectively targeting αvβ6 integrin-expressing solid tumours with minimal off-target effects that restrict current Ad5-based

277 therapies [3]. In addition, $Ad5_{NULL}$-A20 has the potential to be delivered intravenously widening its
278 therapeutic potential for the treatment of metastasis which is limited by intra-tumoural delivery [14].

279 Antibody resistance to existing bispecific antibodies targeting a single TAA is currently a significant
280 limitation leading to target cells losing sensitivity in turn resulting in tumour recurrence. $OAd5_{NULL}$-
281 A20.BICA aims to overcome this limitation by targeting two separate tumour antigens $\alpha v\beta 6$ and EGFR
282 simultaneously. Nonetheless, immune escape is still a possibility and exploration of armed OV's in
283 combination with tri-specific T-cell engagers targeting two TAA concurrently[15] or complementary
284 therapies should be explored. Previous research shows the DNA damage response induced by
285 radiotherapy and chemotherapy increases surface expression of NKG2D ligands, enhancing activity of
286 a Herpes virus simplex OV expressing a NKG2Drp bispecific [16]. Such synergistic effects could be
287 exploited by $Ad5_{NULL}$-A20 CD3-NKG2Drp BICA in combination with either radiotherapy or
288 chemotherapy.

289 The activation of a large number of T-cells by BICA represents a challenge to reach optimal therapeutic
290 potential whilst reducing toxic side-effects. Although our data confirms a robust activation of T-cells
291 exposed to CD3-BICA and complete tumour cell killing for all cell lines tested within 24 hours (oncolytic)
292 or 5 days (replication-deficient) (**Fig. 3**) it should be noted that *in vitro* experiments use homogenous
293 cell lines with 100% transduction efficiency, which is unlikely to be achieved in heterogenous tumours.
294 Organoid cultures also saw rapid T-cell mediated killing as early as two days (**Fig. 5**) in all CD3-BICA
295 tested, though more representative of patient samples, we predict a much more measured response
296 *in vivo*. By delivering the CD3-BICA in $Ad5_{NULL}$-A20 directly to the tumour it is highly unlikely enough
297 BICA would be produced locally to induce the toxicities currently seen via continuous systemic delivery.
298 Encouragingly, previous developed Ad5 based vectors containing T-cell targeting BICA [17] have produced
299 promising results undergoing preclinical evaluation: ICOVIR-15K armed with an anti-EGFR × CD3 BiTE
300 [18] and engineered oncolytic group B adenovirus Enadenotucirev (EnAd) armed with an anti-
301 EpCAM × CD3 BiTE [19], paving the way for development of more Adenovirus-based combination

therapies. Like many OVs, $Ad5_{NULL}$-A20 can broaden its therapeutic potential through the design of BICA targeting alternative TAA such as EPCAM and HER2, for applications in cancers that lack EGFR or MICA. As $Ad5_{NULL}$-A20 is inherently more tumour selective at the level of cell recognition we predict increased potency with negligible off-target effects *in vivo*.

NK cells have generated increasing interest as a solid cancer therapeutic target in recent years due their attractive anti-tumour properties, they demonstrate lower toxicity and higher safety than T-cell BICA, and therefore lower CRS and off-target toxicity [20]. For example, an Anti-CD16 × CD33 bispecific antibody for the treatment of myelodysplastic syndrome (MDS) has been reported to eradicate $CD33^+$ MDS cells and targeted $CD33^+$ myeloid-derived suppressor cells resulting in reduced immunosuppression in the TME and enhanced antitumor efficacy [21]. Here, we demonstrate anti-CD16-EGFR BICA produces a NK-mediated cytotoxic effect when expressed in various cancer cell lines *in vitro*, although the resulting NK mediated tumour cell killing is not as potent as seen with the CD3-BICA in replication-deficient transduced cells, we see complete killing with the addition of the oncolytic (**Fig 4**). *Ex vivo* data showed NK cell mediated killing of PDAC organoids over 4 days (**Fig. 6**), twice as much time as CD3-BICA, this more measured response holds promise for a longer lasting more robust immune response at tumour sites suggesting $Ad5_{NULL}$-A20 CD16-BICA has great potential to be an effective, well tolerated therapeutic going forward.

Organoid models show great promise in predicting patient response to treatment [22]. Using these models in combination with immune cells adds another level of complexity, demonstrating $Ad5_{NULL}$-A20-BICA ability to work in synergy with immune cells creating a potent anti-tumour response in a relevant, complex heterogeneous system.

$Ad5_{NULL}$-A20 CD3-NKG2Drp BICA targets MICA on tumour cells. We show $Ad5_{NULL}$-A20 CD3-NKG2Drp BICA increases T-cells activation *in vitro* albeit at lower levels than CD3-EGFR/EGF (**Fig. 3**) which correlates with lower MICA expression on the cell lines tested in this study (**Fig. S1**). Interestingly, we also saw consistent tumour cell killing of PDAC organoids *ex vivo* (**Fig. 5**) despite very low levels of

MICA on the organoid surface (**Fig. S5A**) however, detectable levels of soluble MICA in organoid supernatants were present (**Fig S5C**) suggesting MICA is being cleaved from the tumour surface as previously reported in pancreatic cancer [23], which did not appear to impact the BICA functionality. In addition to MICA, NKG2D has several MHC-I-like ligand binding partners including MICB and ULBP1-6, as with MICA, these ligands are typically expressed at low levels on the surface of healthy cells but can be upregulated during oncogenic transformation [2018]. Receptor staining of Organoid cultures with these additional ligands (**Fig.S5B**) showed expression of ULBP2 (>25%) MICA (>10%). PDM36, PDM38 and PDM30 had very low MICA (>2%) however ULBP1, 2 and 4 were detected at low levels (>10%) on both organoids, suggesting CD3-NKG2Drp BICA maybe binding to additional ligands in addition to MICA resulting in T-cell activation. Additionally, we cannot rule out that transduction with $Ad5_{NULL}$-A20 itself may be driving increased expression of NKG2D ligands through the DNA damage response [24]. Overall, we hypothesise that CD3scfv-NKG2Drp could be used to target multiple NKG2D ligands on transformed cells in addition to MICA adding an additional benefit to its therapeutic potential.

Despite the heterogenic nature of the organoid samples the combination of αvβ6 targeting oncolytic virus and EGFR/MICA targeting BICA resulted in >50% regression in organoid viability across the organoid donors tested (**Fig. 5 and Fig. 6**). Tumour regression correlated with an increase in cytokine production evident in both T-cell and NK (**Fig. 5d** and **Fig. 6d**) co-cultures, suggesting that the delivery of the BICA via $Ad5_{NULL}$-A20 to tumours enhances T-cell and NK cytotoxicity. Overall, these experiments point towards $Ad5_{NULL}$-A20.BICA inducing a pro-immunogenic TME with potential to kill tumours devoid of target TAAs αvβ6, EGFR and/or MICA.

Overcoming the hostile TME and stroma surrounding tumours remains a challenge to improve the dissemination of OVs to target tumour cells. Encouragingly research is making promising progress in this area by adopting multiple approaches including delivery of OV via the use of mesenchymal stromal cells [25], targeting the stroma itself with the use of armed OVs [26] and using tumour sensitisers such as histone deacetylase inhibitors [27,28] to enhance OV delivery to target sites. As the delivery of

immunotherapies via OVs improves and moves to the clinic a more refined approach to the delivering of viral transgenes should be explored, such as the use of tumour specific enhancers/promoters to further control gene expression and improve patient safety [27].

In summary, we demonstrate that the local delivery of T-cell or NK cell targeting BICA in combination with $Ad5_{NULL}$-A20 produces an effective anti-tumour response in αvβ6 positive tumours resulting in T-cell and NK cell cytotoxicity and tumour regression. This provides an exciting and potentially highly effective approach to systemically target cancer immunotherapies whilst overcoming the limitations associated with the current systemic delivery of BICA. As $OAd5_{NULL}$-A20 heads to clinical trials it will be of great interest to see how combination therapies using this method of delivery develop in the future and how they will best fit into current treatment regimes. $Ad5_{NULL}$-A20.BICA shows promise as a potent Viro-immunotherapy that could be readily transferred to the clinic in the near future.

Material and Methods

Cell culture

T-Rex-293, HEK293-β6, HF-CAR, SKBR3, A431, UMSCC4, PT45 were maintained in DMEM. U373-MICA YFP KYSE30, Panc0403, Jurkat NFκB GFP reporter cells were maintained in RPMI 1640 (Sigma). CHO-K1 were maintained in DMEM-F-12 media and BT20 in MEM, alpha modification (Sigma). Basal media was supplemented with 10% Fetal bovine serum (FBS), heat inactivated, 1% L-Glutamine (200mM stock), 2% Penicillin and Streptomycin (Sigma). CHO expressing EGFR (CHO-EGFR) were generated in-house using Flp-in system (Invitrogen) and maintained with the addition of 500μg/mL Hygromycin (Invitrogen) and 293-β6 with the addition of 1.25μg/mL puromycin (Sigma). See **Table S1** for additional cell line characteristics.

Immune cell Isolation

Apheresis cones obtained from Welsh Blood Service (Talbot Green, South Wales) were processed by layering whole blood onto Ficoll-plaque Plus (Cyvita) following manufacturer's instructions. Immune

cell isolation was carried out using Magnetic Activating Cell Sorting (MACS) using MACS isolated CD3+ T-cells (Miltenyi - Pan T-cell isolation kit) or NK cells (Miltenyi-NK isolation kit) and cultured in supplemented RPMI plus IL-2 or IL-15, respectively.

Generation of viral vectors

Constructs were designed in Snapgene software (v6.2.1) **Table S1** and plasmids generated by Thermoscientific. $Ad5_{NULL}$-A20 bacterial artificial chromosome (BAC) was generated previously in-house [3] **(Table S2)**. BICA were incorporated into the $Ad5_{NULL}$-A20 E1/E1A region using AdZ recombineering as previously described [3,7]. Viral titres were determined by MicroBCA (1μg protein = $4x10^9$ vp) (ThermoScientific), plaque assay and Nanosight technology (NS300, Malvern).

Cell receptor staining

A total of 100,000 cells were stained with primary antibodies human anti-αvβ6 (Millipore), anti-MICA (Origene), anti-EGFR-PE (Biolegend), and appropriate IgG Isotype controls (IgG1 Abcam, IgG2a-PE Biolegend) for 1 hour on ice. Where relevant, secondary antibody Alexa 647 labelled goat anti-mouse $F(ab')^2$ (Life Technologies) was applied to cells (1 hour, on ice), prior to fixation in 4% paraformaldehyde (PFA) (Sigma) and analysed by Flow Cytometry (Accuri C6, BD).

Cell viability assays

25,000 cells were transduced with a dilution (100-5000 virus particles per cell (vp)/cell) of oncolytic $Ad5_{NULL}$-A20 with or without BICA transgenes and incubated for 5 days. To assess immune mediated killing of cancer cells 25,000 cells/well were transduced with $Ad5_{NULL}$-A20 bispecific 2000 vp/cell (replication-deficient) or 500 vp/cell (Oncolytic). Virus was removed and replaced with complete media after 3 hours. After 48 hours purified CD3+ or NK cells were added to the transduced cells and incubated for a further 24- 120 hours. Cell viability was determined by CellTiter-Glo® luminescent cell viability assay (Promega).

Immunogenicity Assays

Cells were seeded at 20,000 cells/well and transduced with 5000 vp/cell $OAd5_{NULL}$-A20-BICA. Extracellular Adenosine triphosphate (ATP) release was detected by addition of RealTime-Glo™ extracellular ATP release assay reagent (Promega) and readings taken every 6 hours. HMGB1 release was calculated using Lumit® High mobility group box 1 (HMGB1) immunoassay (Promega) at 24 hours post-transduction.

Western Blotting

HF-CAR cells were transduced with replication-deficient Ad5-BICA (MOI 10) for 72 hours. Supernatants were collected and cell lysate generated by lysing cell pellets in RIPA buffer (Thermoscientific). Samples were run on 4-12% Bis-Tris NuPAGE gel (Thermo) and transferred to Nitrocellulose membrane (GE Healthcare) and blocked before addition of either anti-V5 tag (Biorad), anti-MICA (Origene), anti-EGF (RnDSystems), or anti-NKG2D (ThermoScientific) antibodies. Primary antibodies were detected with an anti-mouse-IgG linked Horseradish Peroxidase (HRP) secondary antibody (Merck). Membranes containing lysate samples were re-probed with anti-Actin (BioRad) followed by Rabbit anti-IgG-HRP (BioRad). Protein densitometry was performed using ImageJ (v1.45). Lysate displayed as relative abundance to Actin loading control.

EGFR/MICA binding assay

CHOK1 (EGFR-ve) and A431 (EGFR+ve) cells were incubated with CD3-EGFRscfvs, CD16-EGFRscfvs, EGFR-NKG2Dscfvs supernatants containing secreted BICA molecules for 1 hour on ice followed by addition of an anti-V5 tag antibody and an anti-mouse secondary labelled with Alexa Fluor 647. Alternatively, EGFRscfv-MICA and EGF-MICA were incubated on CHOK1/CHO-EGFR cells and detected via an Anti-MICA antibody (Origene). In the instance of CD3scfv-EGF, CD16scfv-EGF, NKG2Dscfv-EGF, 0.5ug of His-tagged recombinant CD3, CD16 or NKG2D (Acro Biosystems) replaced primary antibodies followed by Anti-His Alexa fluor 647 (Biolegend). MICA +/- cells (SKBR3 and U373-MICA respectively) were incubated with CD3scfv-NKG2Drpand CD16scfv-NKG2Drp supernatants before addition of corresponding recombinant protein. Labelled cells were detected via flow cytometry.

425 **Jurkat NFκB GFP reporter assay**

426 25,000 tumour cells were co-cultured with Jurkat NFκB green fluorescent protein (GFP) reporter cells
427 (Systems Biosciences) with an effector-to-target ratio of 1:5 (E:T 1:5) in presence supernatants
428 containing secreted CD3-BICA from transduced cells, for 24 hours. Dynabeads CD3/CD28 (Gibco) were
429 used as a positive control (1:1 ratio). Percentage of GFP positive cells were determined by flow
430 cytometry.

431 **NK CD107a Assay**

432 25,000 CHOK1/CHO-EGFR were co-cultured with NK cell lines [29], (E:T 1:2) in the presence of
433 supernatants containing secreted NK-BICA for 6 hours with CD107a-FITC (Biolegend), Golgi-Plug (BD)
434 and GolgiStop (BD). Cell activation cocktail (Biolegend) was added to positive control wells at 1:50. NK
435 cells were stained with LIVE/DEAD Aqua stain (Invitrogen), CD56-BV605 (Biolegend) and fixed in 4%
436 PFA. For Peripheral Blood Mononuclear Cell (PBMC) co-culture assays a total of 50,000 cells in a 24
437 well plate were transduced with $Ad5_{NULL}$-A20 BICA (replication-deficient at 2000 vp/cell or Oncolytic at
438 500 vp/cell). After 72 hours cells were co-cultured with PBMC (E:T 1:10) or isolated NK cells (E:T 1:2)
439 and CD107a as above and PBMC stained with LIVE/DEAD fixable Aqua, CD14-BV510, CD19-BV510,
440 CD3-BV711, CD56-BV506 before analysis by flow cytometry.

441

442 **T-cell Assays**

443 A total of 25,000 cells were transduced with $Ad5_{NULL}$-A20 CD3-BICA at 2000 vp/cell (replication-
444 deficient) or 500 vp/cell (Oncolytic) for 48 hours. CD3+ T-cells were added at E:T 1:5. Dynabeads
445 Human T-Activator CD3/CD28 (Life tech) were used as a positive control at a 1:1 ratio unless otherwise
446 stated. T-cells were stained with LIVE/DEAD fixable Aqua stain, anti-CD3-PECy7, anti-CD4-FITC, anti-
447 CD8-PEFire700, anti-CD25BV711, and anti-CD69-Alexa-Fluor-647 (AF647) (Biolegend) in activation
448 assays. Intracellular Interferon gamma (IFNγ) assays co-cultured T-cells for 6 hours in the presence of

Brefeldin A (Golgi-Plug, BD). Cell-Activation Cocktail (Biolegend) was added to control wells at 1:50. T-cells were stained with LIVE/DEAD Aqua, anti-CD3-PECy7, anti-CD4-FITC, anti-CD8-PEFire700 followed by fixation and permeabilization using the BD Cytofix/Cytoperm kit (Invitrogen) before addition of anti-IFNγ-APC (Biolegend). To monitor T-cell proliferation CD3+ T-cells were pre-incubated with Cell Trace Far red cell proliferation kit (Invitrogen) prior to co-culture for 5 days**.** All samples were analysed by flow cytometry.

Flow cytometry analysis

All raw data obtained from Attune NxT and Accuri C6 was analysed using FlowJo V.10 software. Cells were gated on single cells using LIVE/DEAD followed by gating on lineage markers were applicable. Fluorescence minus one (FMO) or Isotype controls were used as reference for setting the gates. T-cell proliferation was analysed using Flowjo cell proliferation function and model adapted to best fit of the data. The percentage of cells positive for specific markers or division indexes were plotted in GraphPad Prism software, version 8.1.2.

TNFalpha and IFN gamma ELISA

Cells (25,000 cells/well) were transduced with $Ad5_{NULL}$-A20-BICA before the addition of purified NK cells (E:T 1:2). Supernatants were collected at 48 hours post co-culture. Human Tumour necrosis factor alpha (TNFα) and IFNγ levels were analysed using DuoSet™ ELISA development system (RnDSystems) following manufacturer's instructions.

Patient-derived Organoids

Models and data were derived from the Human Cancer Models Initiative (HCMI) https://ocg.cancer.gov/programs/HCMI; dbGaP accession number phs001486. Pancreatic ductal adenocarcinoma (PDAC) organoids (**Table S5**); were cultured as recommended in ATCC formulation 3 (full media). Receptor staining was carried out on single cell suspensions, EGF was removed from the media 3 days prior to staining. For co-culture assays, organoids were harvested 2-3 days after seeding

(~100uM diameter). Organoids were transduced in suspension with 500-1000 vp/cell $OAd5_{NULL}$-A20-BICA and incubated for 30 minutes at 37 degrees. Isolated CD3+ T-cells (E:T 1:10) or (NK cells E:T 1 :8) were co-cultured with organoids in 30% Matrigel (Corning). Matrigel was allowed to polymerise, then overlaid with full media without EGF. When indicated T-cells were labelled with CFSE cell proliferation dye according to manufacturer's instructions (Life Technologies). Plates were incubated in IncuCyte®S3 (Sartorius). Image acquisition was set for every 3 hours for a duration of between 3 and 5 days. Brightfield images and image analysis was performed either using the IncuCyte® organoid module or standard settings in the presence of fluorescent labelled cells (Sartorius). Luminex xMAP® cytokine custom analysis of co-culture supernatants collected at the end of each experiment was conducted by Indoor Biotechnologies, Inc, Cardiff, UK.

Statistics

Data were analysed using GraphPad Prism (GraphPad Software). Mean and Standard deviation (SD) shown unless otherwise stated. Two-way ANOVA Mult comparison with Dunnett's test to compare treatments was used unless otherwise stated. **p<0.01, ***p<0.001, ****p<0.0001, ns = non-significant.

Data availability

Data is available within the manuscript and upon reasonable request from the corresponding author.

Acknowledgements

The authors are grateful to Professor Richard Stanton for providing access to Incuyte, HF-CAR cells and general recombineering advice. Dr Ceri Fielding for providing MICA/B, ULBP antibodies and U373-MICA YFP cells, MICA advice. Professor Arwyn Jones for providing A431 and SKBR3 cells (All at Cardiff University, Cardiff, UK). Indoor Biotechnologies for conducting Luminex analysis of samples. Graphical abstract and Figure 1A were created in BioRender.com (figure codes: p6qzru4 and h74ic82

respectively). Anonymous healthy donor blood was acquired from Welsh Blood Service and used under local University ethics approval. Funding provided by Cancer Research UK Biotherapeutic Programme award to ALP (C52915/A29104) and Cancer Research UK Experimental Cancer Medicine Centre award to Cardiff University (C7838/A25173).

Author Contributions

RJB: conceptualisation, methodology, visualisation, investigation, formal analysis, writing-original draft, and editing. LMB: investigation, methodology, formal analysis, editing. SK: methodology, investigation, editing. JD: conceptualisation, methodology, investigation. AR: investigation. MP: investigation, ALP: conceptualisation, visualisation, resources, funding acquisition, writing-original draft and editing, study supervision.

Declaration of interests

A.L.P is CSO of Trocept Therapeutics, part of Accession Therapeutics Ltd. All other authors have no COI to declare.

Keywords: Immunotherapy, αvβ6 integrin, Oncolytic, Virotherapy, Bispecific antibody, T-cell, NK cell, solid cancers, Organoid.

References

1. Giraldo, N.A., Sanchez-Salas, R., Peske, J.D., Vano, Y., Becht, E., Petitprez, F., Validire, P., Ingels, A., Cathelineau, X., Fridman, W.H., et al. (2019). The clinical role of the TME in solid cancer. Br. J. Cancer *120*, 45–53.

2. Shalhout, S.Z., Miller, D.M., Emerick, K.S., and Kaufman, H.L. (2023). Therapy with oncolytic viruses: progress and challenges. Nat. Rev. Clin. Oncol. *20*, 160–177.

3. Uusi-Kerttula, H., Davies, J.A., Thompson, J.M., Wongthida, P., Evgin, L., Shim, K.G., Bradshaw, A., Baker, A.T., Rizkallah, P.J., Jones, R., et al. (2018). Ad5NULL-A20: A Tropism-Modified, αvβ6 Integrin-Selective Oncolytic Adenovirus for Epithelial Ovarian Cancer Therapies. Clin. Cancer Res. *24*, 4215–4224.

4. Wang, S., Chen, K., Lei, Q., Ma, P., Yuan, A.Q., Zhao, Y., Jiang, Y., Fang, H., Xing, S., Fang, Y., et al. (2021). The state of the art of bispecific antibodies for treating human malignancies. EMBO Mol. Med. *13*, e14291.

5. Paredes-Moscosso, S.R., and Nathwani, A.C. (2024). 10 years of BiTE immunotherapy: an overview with a focus on pancreatic cancer. Front. Oncol. *14*, 1429330.

6. Goebeler, M.-E., and Bargou, R.C. (2020). T cell-engaging therapies - BiTEs and beyond. Nat. Rev. Clin. Oncol. *17*, 418–434.

7. Stanton, R.J., McSharry, B.P., Armstrong, M., Tomasec, P., and Wilkinson, G.W.G. (2008). Re-engineering adenovirus vector systems to enable high-throughput analyses of gene function. BioTechniques *45*, 659–62, 664.

8. Ma, J., Mo, Y., Tang, M., Shen, J., Qi, Y., Zhao, W., Huang, Y., Xu, Y., and Qian, C. (2021). Bispecific antibodies: from research to clinical application. Front. Immunol. *12*, 626616.

9. Kontermann, R.E., and Brinkmann, U. (2015). Bispecific antibodies. Drug Discov. Today *20*, 838–847.

10. Ayyar, B.V., Arora, S., and O'Kennedy, R. (2016). Coming-of-Age of Antibodies in Cancer Therapeutics. Trends Pharmacol. Sci. *37*, 1009–1028.

11. Fan, G., Wang, Z., Hao, M., and Li, J. (2015). Bispecific antibodies and their applications. J. Hematol. Oncol. *8*, 130.

12. Hosseini, I., Gadkar, K., Stefanich, E., Li, C.-C., Sun, L.L., Chu, Y.-W., and Ramanujan, S. (2020). Mitigating the risk of cytokine release syndrome in a Phase I trial of CD20/CD3 bispecific antibody mosunetuzumab in NHL: impact of translational system modeling. NPJ Syst. Biol. Appl. *6*, 28.

13. Abdeldaim, D.T., and Schindowski, K. (2023). Fc-Engineered Therapeutic Antibodies: Recent Advances and Future Directions. Pharmaceutics *15*.

14. Davies, J.A., Marlow, G., Uusi-Kerttula, H.K., Seaton, G., Piggott, L., Badder, L.M., Clarkson, R.W.E., Chester, J.D., and Parker, A.L. (2021). Efficient Intravenous Tumor Targeting Using the αvβ6 Integrin-Selective Precision Virotherapy Ad5NULL-A20. Viruses *13*.

15. Banaszek, A., Bumm, T.G.P., Nowotny, B., Geis, M., Jacob, K., Wölfl, M., Trebing, J., Kucka, K., Kouhestani, D., Gogishvili, T., et al. (2019). On-target restoration of a split T cell-engaging antibody for precision immunotherapy. Nat. Commun. *10*, 5387.

16. Baugh, R., Khalique, H., Page, E., Lei-Rossmann, J., Wan, P.K.-T., Johanssen, T., Ebner, D., Ansorge, O., and Seymour, L.W. (2024). Targeting NKG2D ligands in glioblastoma with a bispecific T-cell engager is augmented with conventional therapy and enhances oncolytic virotherapy of glioma stem-like cells. J. Immunother. Cancer *12*.

17. Teijeira Crespo, A., Burnell, S., Capitani, L., Bayliss, R., Moses, E., Mason, G.H., Davies, J.A., Godkin, A.J., Gallimore, A.M., and Parker, A.L. (2021). Pouring petrol on the flames: Using oncolytic virotherapies to enhance tumour immunogenicity. Immunology *163*, 389–398.

18. Fajardo, C.A., Guedan, S., Rojas, L.A., Moreno, R., Arias-Badia, M., de Sostoa, J., June, C.H., and Alemany, R. (2017). Oncolytic Adenoviral Delivery of an EGFR-Targeting T-cell Engager Improves Antitumor Efficacy. Cancer Res. *77*, 2052–2063.

19. Freedman, J.D., Hagel, J., Scott, E.M., Psallidas, I., Gupta, A., Spiers, L., Miller, P., Kanellakis, N., Ashfield, R., Fisher, K.D., et al. (2017). Oncolytic adenovirus expressing bispecific antibody targets T-cell cytotoxicity in cancer biopsies. EMBO Mol. Med. *9*, 1067–1087.

20. Demaria, O., Gauthier, L., Debroas, G., and Vivier, E. (2021). Natural killer cell engagers in cancer immunotherapy: Next generation of immuno-oncology treatments. Eur. J. Immunol. *51*, 1934–1942.

21. Gleason, M.K., Ross, J.A., Warlick, E.D., Lund, T.C., Verneris, M.R., Wiernik, A., Spellman, S., Haagenson, M.D., Lenvik, A.J., Litzow, M.R., et al. (2014). CD16xCD33 bispecific killer cell engager (BiKE) activates NK cells against primary MDS and MDSC CD33+ targets. Blood *123*, 3016–3026.

22. Verduin, M., Hoeben, A., De Ruysscher, D., and Vooijs, M. (2021). Patient-Derived Cancer Organoids as Predictors of Treatment Response. Front. Oncol. *11*, 641980.

23. Onyeaghala, G., Nelson, H.H., Thyagarajan, B., Linabery, A.M., Panoskaltsis-Mortari, A., Gross, M., Anderson, K.E., and Prizment, A.E. (2017). Soluble MICA is elevated in pancreatic cancer: Results from a population based case-control study. Mol. Carcinog. *56*, 2158–2164.

24. Cerboni, C., Fionda, C., Soriani, A., Zingoni, A., Doria, M., Cippitelli, M., and Santoni, A. (2014). The DNA Damage Response: A Common Pathway in the Regulation of NKG2D and DNAM-1 Ligand Expression in Normal, Infected, and Cancer Cells. Front. Immunol. *4*, 508.

25. McKenna, M.K., Englisch, A., Brenner, B., Smith, T., Hoyos, V., Suzuki, M., and Brenner, M.K. (2021). Mesenchymal stromal cell delivery of oncolytic immunotherapy improves CAR-T cell antitumor activity. Mol. Ther. 29, 3529–3533.

26. Freedman, J.D., Duffy, M.R., Lei-Rossmann, J., Muntzer, A., Scott, E.M., Hagel, J., Campo, L., Bryant, R.J., Verrill, C., Lambert, A., et al. (2018). An Oncolytic Virus Expressing a T-cell Engager Simultaneously Targets Cancer and Immunosuppressive Stromal Cells. Cancer Res. *78*, 6852–6865.

27. Swift, E.A., Pollard, S.M., and Parker, A.L. (2022). Engineering Cancer Selective Virotherapies: Are the Pieces of the Puzzle Falling into Place? Hum. Gene Ther. *33*, 1109–1120.

28. Diallo, J.-S., Le Boeuf, F., Lai, F., Cox, J., Vaha-Koskela, M., Abdelbary, H., MacTavish, H., Waite, K., Falls, T., Wang, J., et al. (2010). A high-throughput pharmacoviral approach identifies novel oncolytic virus sensitizers. Mol. Ther. *18*, 1123–1129.

29. Rubina, A., Patel, M., Nightingale, K., Potts, M., Fielding, C.A., Kollnberger, S., Lau, B., Ladell, K., Miners, K.L., Nichols, J., et al. (2023). ADAM17 targeting by human cytomegalovirus remodels the cell surface proteome to simultaneously regulate multiple immune pathways. Proc Natl Acad Sci USA *120*, e2303155120.

600 **Figure Legends**

601 **Figure 1. Incorporation of bispecific molecules into precision virotherapies does not affect oncolytic**
602 **properties of OAd5$_{NULL}$-A20**. **(A)** A schematic of the bispecific molecules inserted into Ad5$_{NULL}$-A20
603 virotherapy. **(B-D)** Comparison of oncolytic killing by OAd5$_{NULL}$-A20-BICA in KYSE30 (αvβ6+) (**b**),
604 Panc0403 (αvβ6+) **(C)** and PT45 (αvβ6-) cells **(D)**. Mean and ±SD of triplicates shown. Luminescence
605 relative light units (RLU). **(E-F).** The detection of HMGB1 **(E)** from transduced BT20 (αvβ6+) cells,
606 absolute values shown from an average of triplicates read from standard curve **(F)**. Extracellular ATP
607 release from UMSCC4 (αvβ6+) cells between 42-96 hours, luminescence read out (RLU). Mean of
608 triplicate values shown.

609 **Figure 2. Secreted BICA bind to EGFR/MICA positive cells and activate immune cells**. **(A)** Western blot
610 analysis of the expression and secretion of BICA constructs. **(B)** Binding of BICA to target tumour
611 antigens. CHOK1 (EGFR-ve) and A341 (EGFR+) or CHO-EGFR (EGFR+) and SKBR3 (MICA-ve) and U373-
612 MICA (MICA +ve) were incubated with BICA supernatants prior to addition of corresponding labelled
613 recombinant protein or antibody; fluorescent signal was detected via flow cytometry. **(C-D)** CD3-BICA
614 induce activation of Jurkat NFκB GFP reporter cells. (**c**) Percentage of GFP +ve Jurkat NFκB cells co-
615 cultured with CD3-BICA supernatants in CHOK1 (EGFR-ve) and CHO-EGFR (EGFR+ve) cells. CD3/CD28
616 antibody beads are used as a positive control. An off-target BICA (CD16-EGFRscfvs) was used as a
617 negative control. Mean and ±SD shown (n=3), ****p<0.0001, ns = non-significant. **(D)** Percentage of
618 GFP +ve Jurkat NFκB cells co-cultured with CD3-BICA supernatants in SKBR3 (MICA-ve) and U373-MICA
619 (MICA+ve) cells. CD3/CD28 antibody beads were used as a positive control. An off-target bispecific
620 supernatant (CD16scfv-NKG2Drp) was used as a negative control. Mean and ±SD of individual values
621 shown (n=3). ****p<0.0001, ns = non-significant. **(E)** NK targeting BICA induce activation of NK cells.
622 Percentage of CD107a positive NK cells co-cultured in the presence of CD16-BICA supernatants in
623 CHOK1 (EGFR-ve) and CHO-EGFR (EGFR+ve) cells. Cell activation cocktail was used as a positive control.

An off-target BICA (CD3-EGFRscfvs) was used as a negative control. Mean and ±SD shown of triplicates (n=2). ****p<0.0001, ns = non-significant.

Figure 3. $Ad5_{NULL}$-A20 expressing CD3-BICA induce T-cell activation and immune mediated killing of cancer cells. (A-B). CD4+ and CD8 T-cell activation by CD3-BICA in BT20, KYSE30 and Panc0403. CD3+ T-cells were co-cultured with $Ad5_{NULL}$-A20 CD3-BICA transduced cancer cells and percentage of CD25 and CD69 positive CD4+ **(A)** and CD8+ **(B)** T-cell subsets measured by flow cytometry. **(C)** Intracellular IFNγ. Percentage of IFNγ positive T-cells 48 hours post co-culture. **(D)** T-cell proliferation. Measured over for 5 days by CD3+ T-cells pre-loaded with proliferation dye and analysed by flow cytometry. Cell division index of CD3+ T-cells was calculated using Flowjo software. All experiments **(A-D**) performed in two independent donors: one representative donor shown. Mean and ±SD of triplicates shown. **(E and F)**. Immune cell mediated killing of cancer cell lines expressing BICA. Cell viability of transduced cells with $Ad5_{NULL}$-A20 CD3-BICA co-cultured with CD3+ T-cells. $Ad5_{NULL}$-A20 replication-deficient 1-5 days **(E)** and oncolytic **(F)** 1-2 days post co-culture. Viability normalised to untreated. Experiments performed in two independent donors: one representative donor shown. Mean and ±SD of triplicates repeats shown. Statistical significance was assessed versus untreated cells by two-way ANOVA followed by Dunnett's post hoc analysis for **(A-C**) and one-way ANOVA followed by Dunnett's post hoc test for **(D-F)** (ns p>0.05, *p<0.05, **p<0.01, ***p<0.001, ****p<0.0001). RD= Replication-deficient, Onc = Oncolytic.

Figure 4. $Ad5_{NULL}$-A20 expressing CD16-BICA induce NK cytotoxicity and immune mediated killing of cancer cells. (A). NK cytotoxicity. Percentage of CD56+ CD107+ PBMC co-cultured with $Ad5_{NULL}$-A20 CD16-BICA transduced BT20, KYSE30 and PAnc0403, analysis of the NK cell subset by flow cytometry. Experiments performed in two independent donors: one representative donor shown. Mean and ±SD of triplicates shown. IFNγ **(B)** and TNFα **(C)** production in supernatants of cancer cells transduced with $Ad5_{NULL}$-A20 CD16-BICA and co-cultured with PBMC. (**D-E)**. NK cell mediated killing of cancer cell lines transduced with $Ad5_{NULL}$-A20 CD16-BICA. Cell viability of cancer cells expressing CD16-BICA and co-

cultured with NK cells. $Ad5_{NULL}$-A20 replication-deficient, 1-5 days post co-culture **(D)** and oncolytic 1-2 days post co-culture, performed as two independent experiments **(E)**. Viability normalised to untreated. Experiments performed in two independent donors: one representative donor shown. Mean and ±SD of triplicates repeats shown. Statistical significance was assessed versus untreated cells one-way ANOVA followed by Dunnett's post hoc test for **(A, D, and E)** (ns p>0.05, *p<0.05, **p<0.01, ***p<0.001, ****p<0.0001). RD= Replication-deficient, Onc = Oncolytic.

Figure 5. **$Ad5_{NULL}$-A20 expressing CD3-BICA promote T-cell mediated killing of patient derived pancreatic organoids. (A)** Representative Incucyte images of pancreatic organoids transduced with $OAd5_{NULL}$-A20 or $OAd5_{NULL}$-A20 CD3-EGFRscfvs, CD3scfv-EGF and CD3scfv-NKG2Drp in co-culture with CD3+ T-cells 2 days post-infection. Performed in 2 independent donors, one representative donor shown for each sample. Scale bar = 100µm. **(B)** Incucyte analysis of organoid integrity using a measure of 'Roundness' in **(A)**. 0= round/maximum integrity. One-way ANOVA was used to compare across groups **p<0.01, ***p<0.001, ****p<0.0001, ns = non-significant. **(C).** Measure of cell viability at 72 hours post co-culture. Performed in 2 independent donors, one representative donor shown for each sample. Mean ±SD of triplicate repeat samples shown. One-way ANOVA followed by Dunnett's post hoc test was used to assess **(C)** (ns p>0.05, *p<0.05, **p<0.01, ***p<0.001, ****p<0.0001). **(D)** Luminex xMAP® multiplex cytokine analysis of PDM38 co-cultures, one representative donor shown. Displayed as a heatmap indicating increases in cytokine production (pg/mL).

Figure 6. **$Ad5_{NULL}$-A20 expressing CD16-BICA promote NK cell mediated killing of patient derived pancreatic organoids. (A).** Representative Incucyte images of pancreatic organoid (PDM38) transduced with $OAd5_{NULL}$-A20 or $OAd5_{NULL}$-A20 CD16-EGFRscfvs, CD16scfv-EGF in co-culture with NK cells (E:T 1:8) at 72 hours post-infection. Two independent NK cell donors shown. **(B)** Incucyte analysis of organoid integrity using a measure of 'Roundness' in (A). 0= round/maximum integrity. One-way ANOVA was used to compare across groups ****p<0.0001. **(C)** Measure of cell viability at 96 hours post co-culture. Shown in 2 independent NK cell donors. Mean ±SD of triplicate repeat samples shown.

674 One-way ANOVA followed by Dunnett's post hoc test was used to assess **(C)** (ns $p>0.05$, *$p<0.05$,
675 **$p<0.01$, ***$p<0.001$, ****$p<0.0001$). **(D)** Luminex xMAP® multiplex cytokine analysis of PDM38 co-
676 cultures, one representative donor shown. Displayed as a heatmap indicating increases in cytokine
677 production (pg/mL).

678

Figure 1

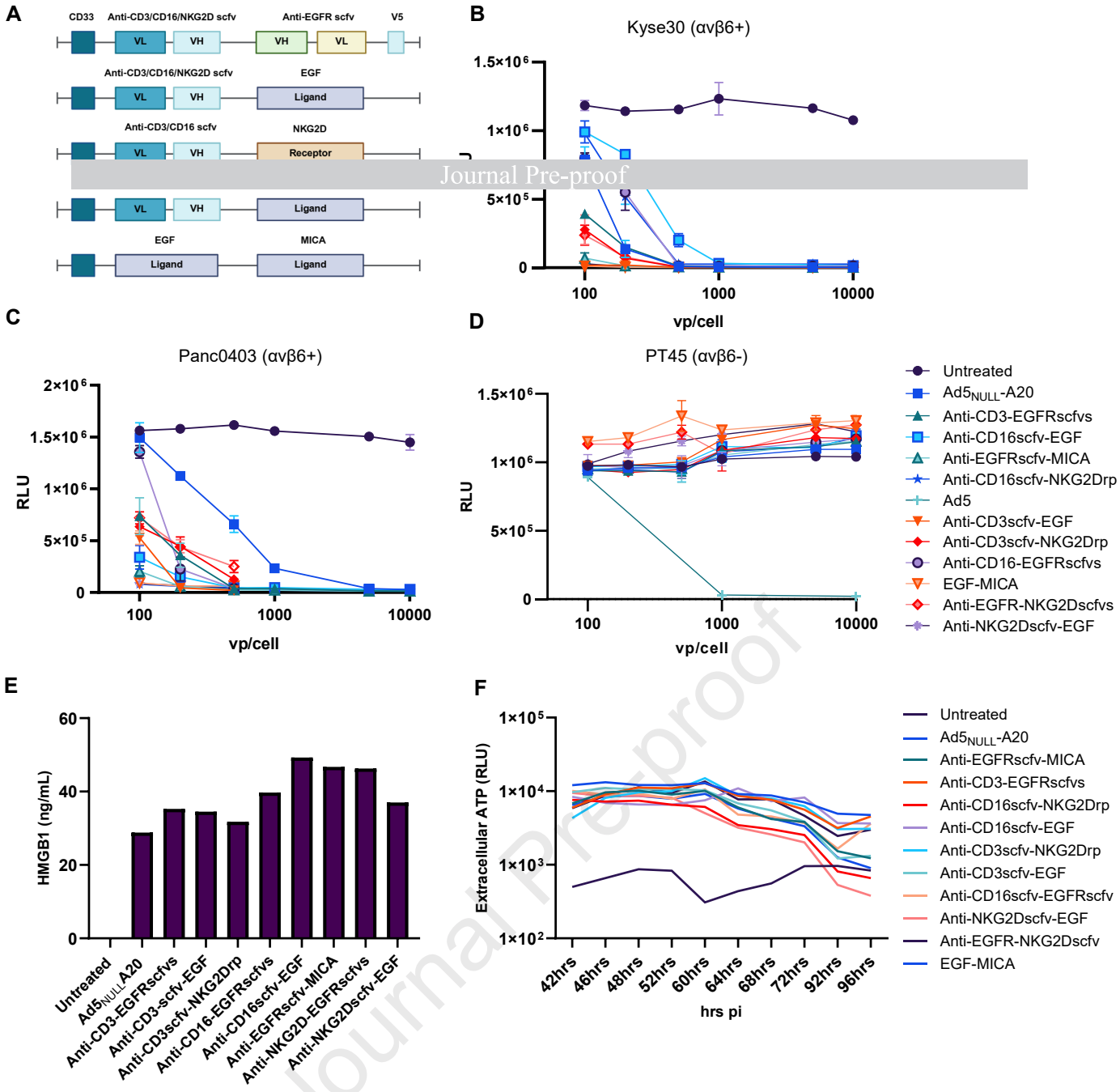

Figure 2

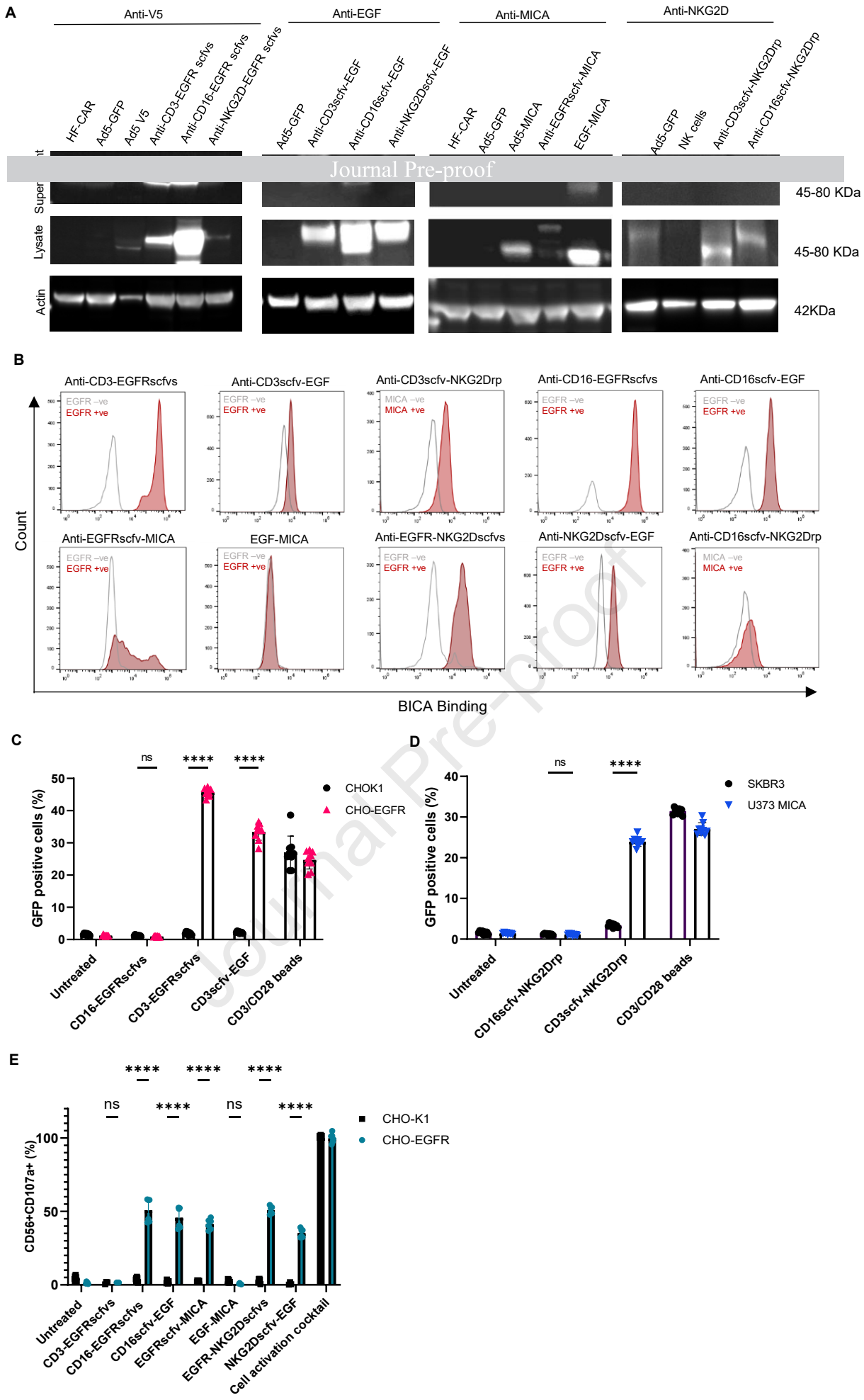
A
Anti-V5
Anti-EGF
Anti-MICA
Anti-NKG2D
HF-CAR
Ad5-GFP
Ad5 V5
Anti-CD3-EGFR scfvs
Anti-CD16-EGFR scfvs
Anti-NKG2D-EGFR scfvs
Ad5-GFP
Anti-CD3scfv-EGF
Anti-CD16scfv-EGF
Anti-NKG2Dscfv-EGF
HF-CAR
Ad5-GFP
Ad5-MICA
Anti-EGFRscfv-MICA
EGF-MICA
Ad5-GFP
NK cells
Anti-CD3scfv-NKG2Drp
Anti-CD16scfv-NKG2Drp
Journal Pre-proof
Super
Lysate
Actin
45-80 KDa
45-80 KDa
42KDa
B
Anti-CD3-EGFRscfvs
Anti-CD3scfv-EGF
Anti-CD3scfv-NKG2Drp
Anti-CD16-EGFRscfvs
Anti-CD16scfv-EGF
Anti-EGFRscfv-MICA
EGF-MICA
Anti-EGFR-NKG2Dscfvs
Anti-NKG2Dscfv-EGF
Anti-CD16scfv-NKG2Drp
EGFR –ve
EGFR +ve
MICA –ve
MICA +ve
Count
BICA Binding
C
GFP positive cells (%)
ns
****
****
CHOK1
CHO-EGFR
Untreated
CD16-EGFRscfvs
CD3-EGFRscfvs
CD3scfv-EGF
CD3/CD28 beads
D
GFP positive cells (%)
ns
****
SKBR3
U373 MICA
Untreated
CD16scfv-NKG2Drp
CD3scfv-NKG2Drp
CD3/CD28 beads
E
CD56+CD107a+ (%)
****
****
****
ns
****
ns
****
CHO-K1
CHO-EGFR
Untreated
CD3-EGFRscfvs
CD16-EGFRscfvs
CD16scfv-EGF
EGFRscfv-MICA
EGF-MICA
EGFR-NKG2Dscfvs
NKG2Dscfv-EGF
Cell activation cocktail

Figure 3

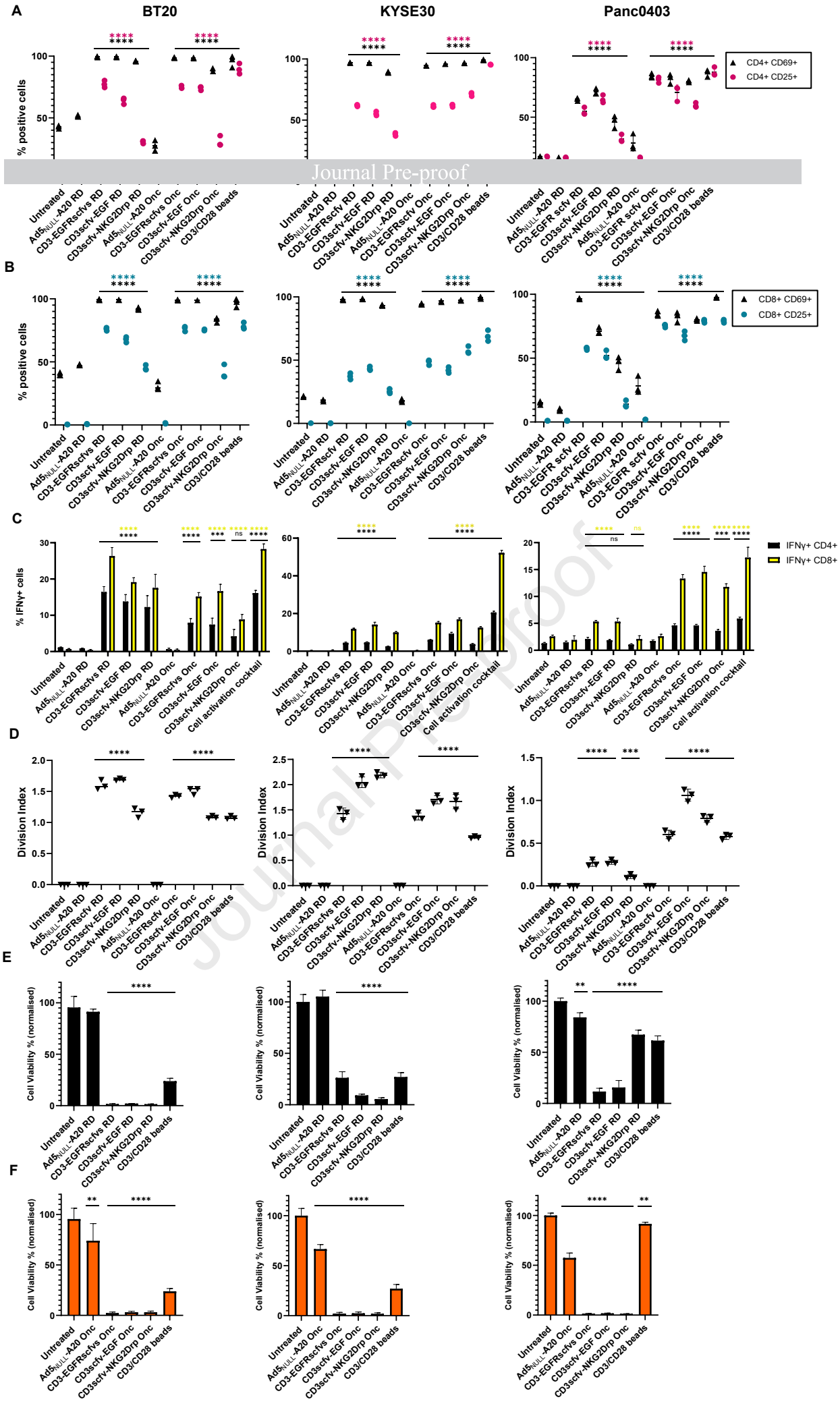

Figure 4

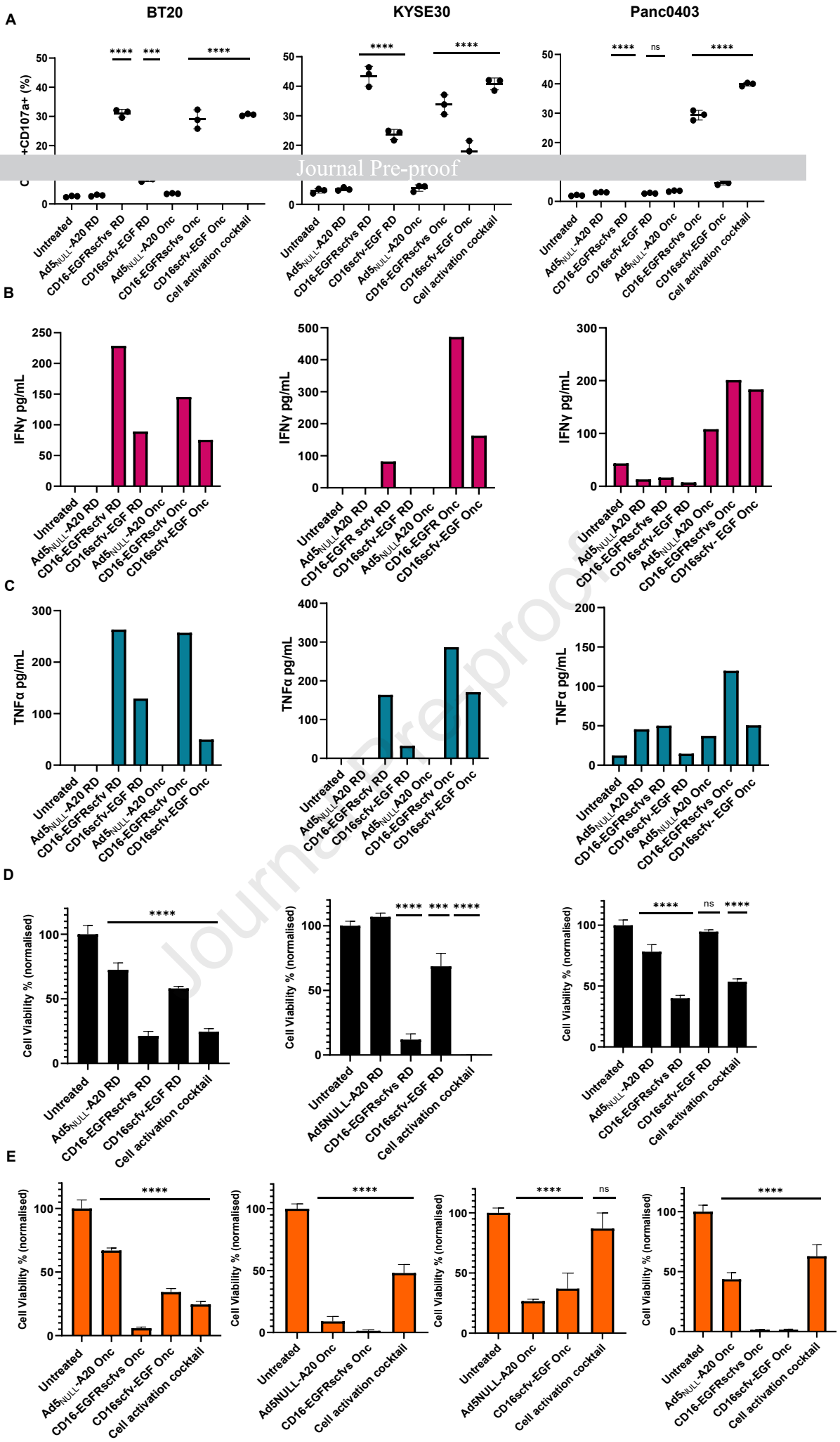
A
BT20
KYSE30
Panc0403
+CD107a+ (%)
Untreated
Ad5NULL-A20 RD
CD16-EGFRscfvs RD
CD16scfv-EGF RD
Ad5NULL-A20 Onc
CD16-EGFRscfvs Onc
CD16scfv-EGF Onc
Cell activation cocktail
B
IFNγ pg/mL
C
TNFα pg/mL
D
Cell Viability % (normalised)
E
Journal Pre-proof

Figure 5

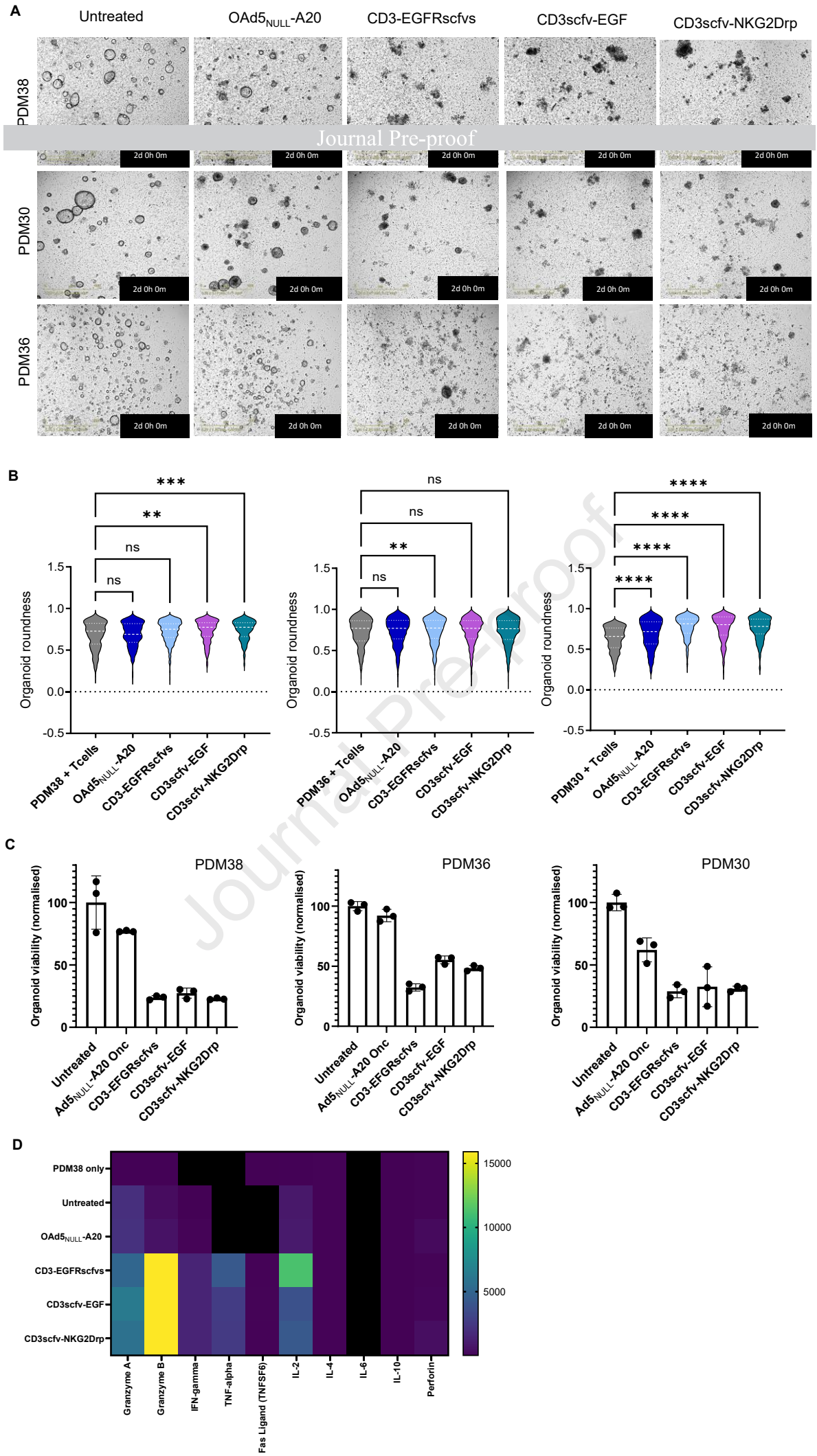

Figure 6

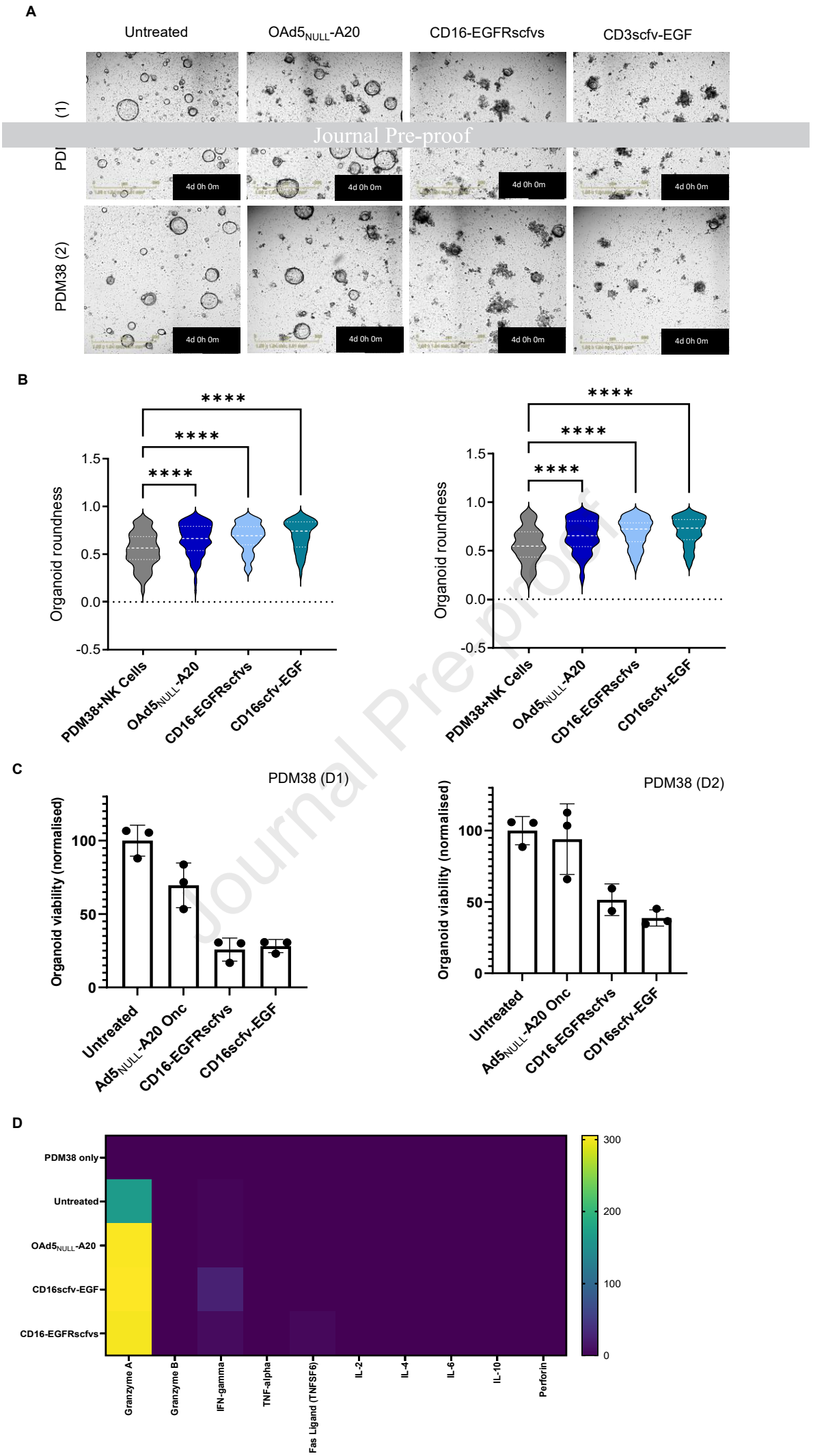

Virotherapies can deliver anti-cancer therapeutics directly to tumours. Bayliss and colleagues develop a precision virotherapy expressing bispecific immunotherapies from tumour cells resulting in immune cell activation and tumour cell killing. Combination cancer therapy has potential to enhance regression of solid tumours in a targeted manner improving on current approaches.